Transport and NMR study of the scandium boron carbide compound $Sc_2B_{1.1}C_{3.2}$ with a boron and carbon mixed graphitelike layer

T. Mori,* M. Tansho, Y. Onoda, Y. Shi, and T. Tanaka
National Institute for Research in Inorganic Materials, Namiki 1-1, Tsukuba 305-0044, Japan
(Received 30 August 1999; revised manuscript received 17 April 2000)

Transport properties and nuclear magnetic resonance (NMR) of the new scandium boron carbide compound $Sc_2B_{1.1}C_{3.2}$ were investigated. $Sc_2B_{1.1}C_{3.2}$ has a trigonal crystal structure [$a=b=23.710(9)A$, $c=6.703(2)A$, $P3m1$] and is composed of alternate [$B_{1/3}C_{2/3}$]-Sc-C-Sc-[$B_{1/3}C_{2/3}$] layers, with the boron and carbon mixed layer [$B_{1/3}C_{2/3}$] forming a very rare graphitelike structure. Physical properties similar to graphite intercalation compounds (GIC) were observed. The temperature dependence of the resistivity showed a large anisotropy. The in-plane resistivity showed a metallic quadratic dependence, also observed in some GIC's while the resistivity along the *c* axis, perpendicular to the layers, increased with decreasing temperature. From magnetic susceptibility and specific-heat measurements, the orbital susceptibility was indicated to take a paramagnetic value. At low temperatures an increase of the in-plane resistivity with $\log T$ dependence and negative magnetoresistance was observed. Two-dimensional Anderson localization was indicated, possibly originating from disorder in the [$B_{1/3}C_{2/3}$] graphitelike layer. ^{11}B magic angle spinning (MAS) nuclear magnetic resonance (NMR) results indicate a large distribution of the chemical shift of the boron nuclei, which is consistent with the existence of disorder within the graphitic layer.

I. INTRODUCTION

Research of the graphite intercalation compounds (GIC) has been extensively carried out since the beginning of the 1970's.[1] From a fundamental standpoint, a countless number of interesting phenomena, such as the appearance of superconductivity, staging, large anisotropy, to name a few, have been discovered. The GIC's are also interesting practically, for example, as new materials for batteries, etc. Quite recently, a new layered material of scandium boron carbide compound $Sc_2B_{1.1}C_{3.2}$, was discovered.[2] The trigonal crystal structure [$a=b=23.710(9)A$, $c=6.703(2)A$, $P3m1$] is composed of alternate [$B_{1/3}C_{2/3}$]-Sc-C-Sc-[$B_{1/3}C_{2/3}$] layers. The structure of $Sc_2B_{1.1}C_{3.2}$ is shown in Fig. 1. A particularly interesting feature of the structure was that the boron and carbon atoms [$B_{1/3}C_{2/3}$] appear to form a puckered graphitelike layer within the compound. To our knowledge, up to now, only three compounds have been reported with the [BC] graphitelike framework, LiBC,[3] MgB_2C_2,[4] and BC_3.[5] Boron and carbon mixed graphitelike layers are very interesting in themselves for the following possible applications; as possible base materials for new fullerenes and possible high-spin molecular magnets, leading to applications as magnetic components.

A striking feature of these compounds is that the scandium-carbon-scandium layers could be removed from the compound with the application of oxydic agents. In other words, the Sc-C-Sc constituents are reminiscent of intercalants in a GIC. Since this compound was synthesized by the solid-state reaction, which is largely different from conventional GIC synthesis, further study on the dynamics of the formation of the graphitelike structure of this compound may lead to the realization of a new family of graphite intercalationlike compounds. In order to investigate the physical properties of this compound, measurements on resistivity, Hall coefficient, specific heat, magnetic susceptibility, and NMR were performed on single crystals. Similar properties to GIC's were indeed observed indicating that this compound can be considered to be a new graphite intercalation-like compound.

II. EXPERIMENT

The $Sc_2B_{1.1}C_{3.2}$ crystals measured were grown and characterized in the following way.[2] First of all, polycrystalline feed rods of $Sc_2B_{1.1}C_{3.2}$ were prepared using Sc_2O_3 powder (4N, Crystal System Inc., Japan), amorphous boron (3N, SB-Boron Inc., U.S.A.) and graphite (3N, Koujundo Kagaku Co., Japan) as starting materials. Sc_2C_{1-x} was synthesized by the carbothermal reduction of scandium oxide under vacuum. The required amount of boron and carbon were added next and synthesized again. Synthesis was performed in a BN crucible surrounded by an inductively heated graphite susceptor at the temperature of 1700 °C. Crystals were grown by the floating zone method in a xenon lamp image furnace, with a growth speed of 2 mm/h. The crystals were characterized by four-circle single-crystal x-ray analyses, chemical analyses, and electron-diffraction microscopy. The existence of multigrains could be seen in the crystals. However, the grains were fairly large, being on the order of millimeter size. The samples used for measurements had the following dimensions; a cylindrical sample with a diameter of 6.2 mm and length of 3.0 mm, and two rectangular flat samples with similar dimensions of $4.7\,\text{mm}\times1.4\,\text{mm}\times0.25\,\text{mm}$. The Laue pattern indicated that the basal plane of the flat samples were perpendicular to the *c* axis.

The in-plane resistivity was determined by using the typical four-probe method. Two different configurations of four-probe measurements were made to obtain the resistivity along the *c* axis. First, a typical method used to measure the *c*-axis resistivity of GIC's was used in which voltage probes

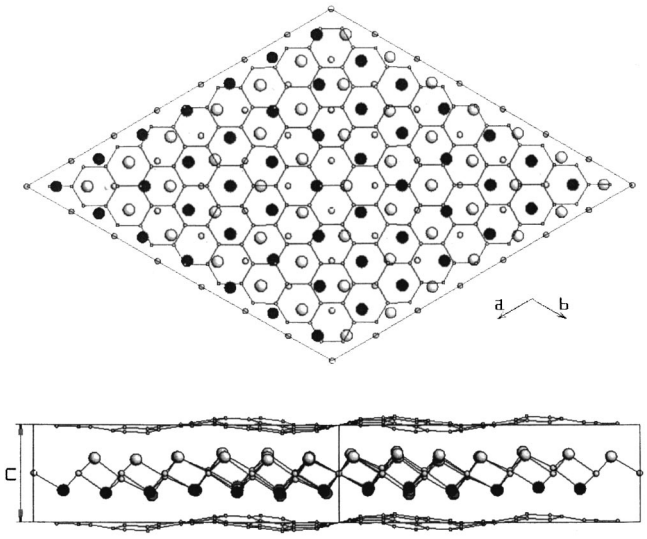

FIG. 1. Structure of $Sc_2B_{1.1}C_{3.2}$ determined from crystallographic measurements. Projection of $Sc_2B_{1.1}C_{3.2}$ structure on a-b plane (top) and (110) plane (bottom). The large open and filled circles represent scandium atoms in different layers. Small open circles represent the boron and carbon mixed layer, while medium open circles indicate $C_{z=1/2}$ atoms.

and current probes are attached to the basal plane of the sample, on opposite sides, aligned along the c axis. However, since in our sample the basal resistivity turned out to have unnegligible values due to a large residual resistivity, a current distribution results within the basal plane, and absolute values of the c-axis resistivity are difficult to obtain. To remove effects of the unnegligible basal resistivity, in the second measurement configuration, both sides of the sample are covered with silver paint and resistivity is measured with four probes. Since the values of resistivity for the c axis were relatively large ($\geqslant$11 mΩ cm), it was judged from previous experience with similar material crystals that any contact resistance between the paint and surface of the sample can be ignored in these magnitudes and the resistivity values given in this configuration correctly represent the c-axis resistivity. Furthermore, an approximate evaluation using data from the first method, which is not dependent of silver paint, also yielded similar absolute values for the c-axis resistivity supporting this conclusion. In order to exclude the resistive voltage caused by any small misalignment of the Hall voltage probes, the magnetic field was varied from -70 kG to 70 kG, and the component linear to the magnetic field was separated from a constant term.

The specific heat was measured by a transient heat pulse method with a small temperature increase of 2% relative to the system temperature. A polished face of a flat sample was attached to an alumina plate holder using Apiezon N grease. Results from a blank run of the holder and grease were subtracted from the data to obtain the specific heat of the sample. The measured temperature region was from 300 to 2 K.

Magnetic susceptibility of the circular sample was measured by using a quantum design superconducting quantum interference device magnetometer from 300 to 2 K.

To prevent surface effects in the NMR experiments, the grown crystal was crushed into powder. NMR measurements

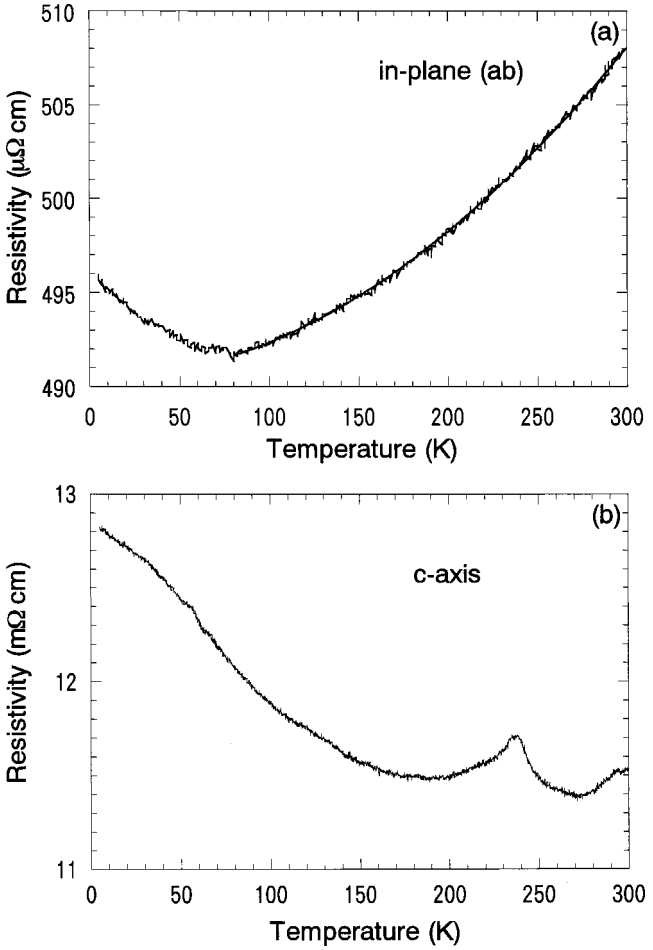

FIG. 2. Temperature dependence of the (a) in-plane resistivity and (b) c-axis resistivity of $Sc_2B_{1.1}C_{3.2}$. The solid curve in (a) indicates the fitted curve of $\rho=\rho_0+\rho_1T^2$.

were conducted at room temperature using a Bruker MSL 400 spectrometer with a magnetic field of 9.4 T. A Doty magic-angle spinning (MAS) probe was used since it has negligible boron background. The powdered sample was packed in 7 mm o.d. zirconia rotors and spinning frequencies of up to 8 kHz were attained. ^{11}B NMR was measured with a saturated H_3BO_3 solution as a reference. The typical $\pi/2$ pulse width for ^{11}B was 3.1 μs. ^{11}B NMR spectra was obtained from Fourier transform of the free induction decays (FID).

III. RESULTS AND DISCUSSION

A. Resistivity

The temperature dependence of the in-plane resistivity is given in Fig. 2(a). A metallic type temperature dependence is observed. As the temperature is lowered from 300 K, the resistivity decreases. The resistivity takes a broad minimum around 80 K and then increases with decreasing temperature. A fit of the temperature dependence of the resistivity between 300 and 80 K as the sum of a temperature-independent term and a polynomial of temperature

$$\rho=\rho_0+\rho_1T^n \tag{1}$$

yielded $n=2.02\pm0.02$. Therefore, since it is indicated that the major conduction mechanism in this temperature region is quadratic, we set $n=2$, and refit the data. We obtain parameters of $\rho_0=490\,\mu\,\Omega$ cm and $\rho_1=2.0\times10^{-10}\,\Omega$ cm/K.^{2} The temperature-independent resistivity takes a large value, which will be discussed in Sec. III C. The calculated curve is shown in the figure as a solid line.

The quadratic temperature dependence of the resistivity has been observed in GIC's and has been attributed to an interpocket electron phonon scattering.[6] From the fitting above, we can conclude that the major temperature-dependent scattering mechanism in this temperature region is not the typical electron-phonon scattering of three-dimensional systems, but rather such an interpocket transition, which reflects the two-dimensional nature of the system. The quadratic temperature dependence indicates that we are observing the conduction pertaining to the graphitelike layers, i.e., there is charge transfer from the scandium atoms and it is not simply conduction of metallic scandium, for example.

A low-temperature upturn of the resistivity is observed around 70 K. The origin of this will also be discussed in Sec. III C.

The temperature dependence of the *c*-axis resistivity is given in Fig. 2(b). In contrast to the in-plane resistivity, the *c*-axis resistivity increases with decreasing temperature. An anomaly is observed at around 240 K and a bend in the curve can be seen around 60 K. Since the anomaly was reproducible for different samples, we think it is not a spurious effect, but that some kind of structural transition may account for this behavior. However, at present it is not clear.

To summarize, we have observed anisotropy in the temperature dependence of the resistivity of $Sc_2B_{1.1}C_{3.2}$. The in-plane resistivity has a metallic quadratic temperature dependence whereas the *c*-axis resistivity increases with decreasing temperature. The anisotropy reflects the layered structure of this compound, which was recently determined by crystallographic methods and is similar to the behavior of some GIC's.

B. Hall effect

The Hall coefficient R_H was determined to be -1.5×10^{-3} cm^3/C at 300 K with the magnetic field parallel to the *c* axis. The negative value indicates that the carriers are electrons. The value corresponds to 4.1×10^{21} carriers/cm^3. This corresponds to 0.14 carriers per Sc atom. Little temperature dependence was observed with 3.6×10^{21} carriers/cm^3 determined for both 80 and 5 K.

Although the band structure of the compound is not clear, the small number of carriers per scandium atom may be due to the fact that the [BC] graphitelike layer is expected to be electron deficient compared to graphite.

C. Magnetoresistance

A broad minimum is observed in the in-plane resistivity [Fig. 2(a)]. To investigate this behavior further we studied the magnetoresistance. In Fig. 3 we compare the resistivity at zero field and the resistivity under a magnetic field of 70 kG applied perpendicular to the basal plane. In the temperature region below 80 K, the resistivity is smaller for 70 kG,

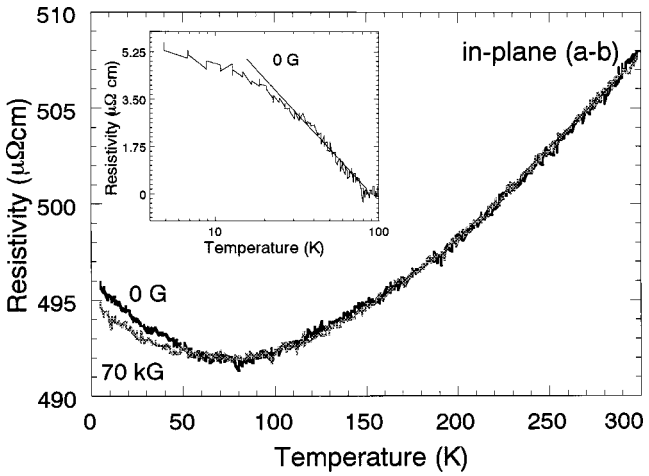

FIG. 3. Temperature dependence of the in-plane resistivity of $Sc_2B_{1.1}C_{3.2}$ at zero field (bold line) and 70 kG (gray line). The zero-field data is the same as that of Fig. 1. The inset figure is the in-plane resistivity below 100 K plotted versus log *T*, after the quadratic and temperature-independent terms determined in Sec. III A have been subtracted. The line is a guide to the eye.

namely, a negative magnetoresistance is observed. Furthermore, in the inset of Fig. 3, we plot the zero-field resistivity at low temperatures versus log *T*, after the quadratic and temperature-independent terms determined in Sec. III A have been subtracted. The increase in resistivity appears to follow a log *T* dependence, with a little saturation at low temperatures. The solid curve is drawn to guide the eye.

We can think of two possibilities to account for the increase in resistivity at lower temperatures and the negative magnetoresistance: (1) the Kondo effect, due to magnetic impurities in the sample,[7] or (2) two-dimensional (2D) Anderson localization in the weakly localized regime, due to disorder in the sample.[8,9]

Since the residual resistivity of our sample ρ_0 is quite large, 490 $\mu\Omega$ cm, and the impurity content not so high (to be given later in Sec. III E), we judge that case (1), the Kondo effect, which is a single magnetic impurity scattering phenomena, is not likely. The unitary limit in the case of *l*-wave scattering is given by[10]

$$\rho_0=c4(2l+1)m/[e^2\pi\hbar D(E_F)], \tag{2}$$

where *c* is the impurity concentration and $D(E_F)$ is the density-of-states at the Fermi energy. We can calculate this using specific-heat data (which will be presented in Sec. III D) to obtain $3(2l+1)\,\mu\Omega$ cm per percent impurity. This is a factor of 3 smaller than the experimental value of 13 mΩ cm per percent impurity we obtain. Therefore, this high value cannot be explained by independent scattering events and the Kondo effect is not likely. The large value of residual resistivity indicates the existence of cooperative phenomena, such as localization, case (1). We note that our crystal is a single crystal with large subgrains and therefore, not much resistance due to grain boundaries is expected, compared to the case of polycrystals.

Furthermore, the idea that appreciable disorder exists in the sample leading to a localized state, was also supported by the structure. X-ray results indicated that the graphitelike layer of boron and carbon atoms is disordered, i.e., bond

lengths could not be assigned to an ordered array of B and C within the plane. This may originate from the fact that the boron carbon composition in the layer is different from the three other compounds with boron carbon graphitelike structures, and actually may not be the optimum composition for an ordered [BC] layer. Previously such 2D weak localization effects have appeared a number of times in similar graphite intercalation compound systems.[11–17] Actually some of these GIC's were judged to be good model systems for studying 2D weak localization.[13,17]

The magnetic-field dependence of the resistivity at 5, 20, and 100 K was measured. While no sizable magnetoresistance is observed at 100 K, negative magnetoresistance is observed at 5 and 20 K. The field dependence of the data at 5 and 20 K was not inconsistent with a H^2 dependence at lower fields and a log H dependence at higher fields, which is expected for 2D Anderson localization in the weakly disordered regime.[18]

Summing up, we attribute the minimum in the resistivity and the negative magnetoresistance to 2D spatial localization of the electronic wave functions. We believe that the origin of this disorder comes from the disordered structure of the [BC] plane. Possibly this is due to the singular composition of B versus C.

D. Specific heat

The specific heat of $Sc_2B_{1.1}C_{3.2}$ is plotted in Fig. 4(a), in the conventional C/T versus T^2 plot in the temperature range between 2 and 42 K. A linear curve is obtained, indicating that the specific heat can be described well as the sum of a linear electronic specific-heat term and phonon T^3 term:

$$C=\gamma T+C_2T^3. \tag{3}$$

The parameters $\gamma=3.59\,\mathrm{mJ\,mol/K^2}$ and $C_2=48.3\,\mu\mathrm{J\,mol/K^4}$ are determined. γ satisfies the relation

$$\gamma=\pi^2/3k_B^2D(E_F). \tag{4}$$

$D(E_F)$ is determined to be $2.3\times10^{22}\,\mathrm{states/eV\,m^3}$. From the coefficient of the phonon term, the Debye temperature $\theta_D=(1.47\times10^3N_Ak_B/C_2)^{1/3}$ is determined to be 633 K. This value is higher than many GIC's, and probably reflects a higher phonon density-of-states at higher energies due to the lighter boron atoms.

E. Magnetic susceptibility

The static magnetic susceptibility of $Sc_2B_{1.1}C_{3.2}$ is given in Fig. 4(b). The magnetic field was applied parallel to the longitudinal axis of the cylindrical sample. This direction is that of the growth direction and was indicated to be ⟨110⟩, which is within the basal plane.

As shown by the solid curve, the data can be fit well as a temperature-independent term χ_0 and Curie-Weiss term. χ_0 took a value of 5.7×10^{-5} emu/mole, while the Curie constant was 1.6×10^{-3} emu/mole K and the Curie-Weiss temperature $\theta=-1.8$ K. We attribute the Curie-Weiss term to magnetic impurities and/or paramagnetic localized spins in the sample. If a single kind of magnetic impurity is assumed, the maximum number of impurities in our sample can be calculated to be $1.3/p^2\%$, where p is the effective number of Bohr magnetons. For example, in the case of iron atomic impurities, this would take a value of 370 ppm.

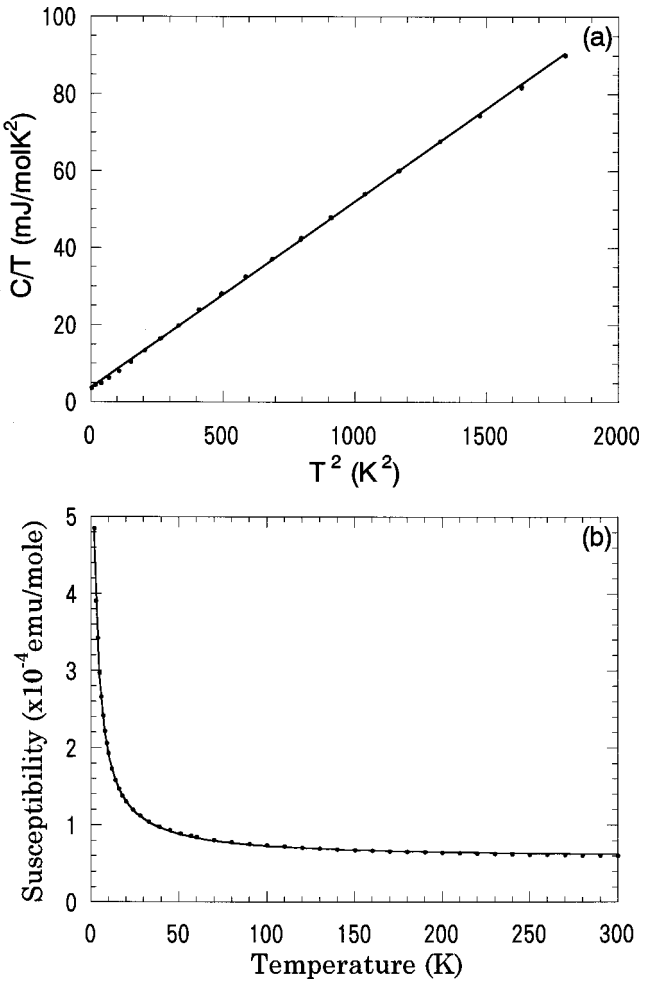

FIG. 4. (a) Specific heat of $Sc_2B_{1.1}C_{3.2}$ shown in the form of the conventional C/T plots as a function of T^2 in the temperature range between 2 and 42 K. The line indicates the fitted curve to Eq. (1), with the parameters $\gamma=3.59\,\mathrm{mJ/\,mol/K^2}$ and $C_2=48.3\,\mu\mathrm{J/\,mol/K^4}$. (b) Temperature dependence of the static magnetic susceptibility of $Sc_2B_{1.1}C_{3.2}$. The solid line indicates the fitted curve as a sum of a temperature independent term and Curie-Weiss term. Parameters are given in the text.

We note that an anomaly in the magnetic susceptibility was not observed at the temperature where the in-plane resistivity goes through a minimum. This could be due to the fact that the transition to localized states is not sharp, as can be seen by the broadness of the minimum in Fig. 2(a).

The total susceptibility χ in these kinds of systems is comprised of

$$\chi=\chi_0+\chi_{orb}+\chi_C+\chi_P, \tag{5}$$

where χ_0 is the diamagnetism from core electrons, χ_{orb} is the interband and intraband orbital susceptibility, χ_C is the Curie (or Curie-Weiss) contribution from paramagnetic spins, and χ_P the Pauli paramagnetism from free carriers. We have already separated χ_C from the total susceptibility as shown in Fig. 4(b). χ_0 is known. χ_P can be estimated from the relation $\chi_P=\mu_B^2D(E_F)$, where μ_B is the Bohr magneton. In this pro-

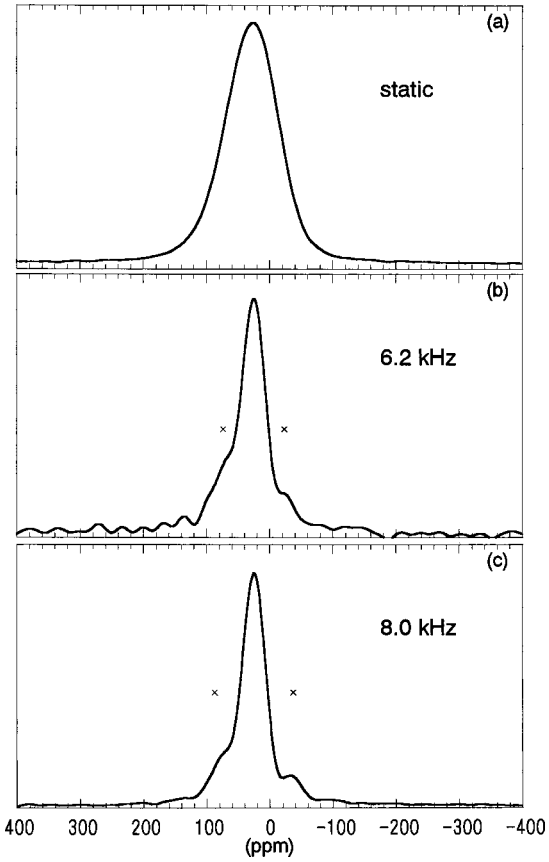

FIG. 5. ^{11}B NMR spectra of $Sc_2B_{1.1}C_{3.2}$ at 128 MHz obtained from Fourier transform (FT) of the FID signals for (a) the static case, and MAS spectra with spinning speeds of (b) 6.2 kHz and (c) 8 kHz. The *x* marks indicate the positions where spinning sidebands are expected to be seen. The shift of the ^{11}B NMR signal is determined relative to the reference signal of saturated H_3BO_3 solution, which is set as 19.49 ppm.

cedure, we ignored effects from electron-phonon enhancement of the specific heat and also the electron-electron enhancement of χ_P.

As a result, we obtain the orbital susceptibility χ_{orb} of $Sc_2B_{1.1}C_{3.2}$ to be $\sim 47\times 10^{-6}$ emu/mole, which is paramagnetic. Orbital paramagnetism has been observed in GIC's. This was attributed to both interband and intraband effects.[19,20] However, it is not clear at present whether the same physical picture applies to $Sc_2B_{1.1}C_{3.2}$.

F. ^{11}B NMR

The static ^{11}B NMR waveform is given in Fig. 5(a). The linewidth of the signal is quite large, being 98 ppm at half-maximum. Upon MAS of the sample at a frequency of 6.2 kHz, a narrowing of the linewidth is observed [Fig. 5(b)]. No sizable further reduction of the linewidth is observed on increasing the spinning frequency to 8 kHz [Fig. 5(c)]. The linewidth is still quite large, being 48 ppm. The linewidth is so large in fact that despite the high-spinning frequencies, the spinning sidebands are partially obscured. We will consider the origins of this large linewidth. The comparison of Figs. 5(b) and 5(c) excludes dipolar broadening as an origin. To evaluate whether the electric quadrupole coupling is a factor of the large linewidth, we will try to evaluate ν_Q, the quadrupole frequency. We assume that the asymmetry parameter is zero. In this case,

$$\nu_Q = e^2 Q_q / 2h, \tag{6}$$

where eQ is the nuclear electric quadrupole moment and eq is the largest principal value of the quadrupole interaction of the electric-field gradient. To first order, weak singularities of the satellite lines should be observed at positions $\pm \nu_Q/2$ from the central peak. Measuring the signal in a wide frequency window, we observe small satellite signals with peaks in positions about $\sim$0.35 MHz apart on either side of the central peak. From this we can estimate ν_Q to be $\sim$0.7 MHz. Broadening of the central peak due to second-order quadrupole interaction is of the order of $25\nu_Q^2/(48\nu_L)$, where ν_L is the measuring frequency, in this case 128.3 MHz. If we use the value of ν_Q determined above, this broadening can be estimated to be $\sim$0.5 kHz (4 ppm). This is much smaller than the linewidth of our signal. There is not expected to be any distribution in the Knight shift of the sample due to itinerant conduction electrons in our sample. Therefore, it is strongly indicated that the relatively large linewidth observed is due to a broad distribution of the chemical shift of the boron nuclei. This indication of a broad distribution of the electronic environment of the boron nuclei is consistent with the existence of disorder concluded from the transport experimental results.

IV. CONCLUSIONS

Physical properties of the layered compound $Sc_2B_{1.1}C_{3.2}$ were investigated. The crystal structure of $Sc_2B_{1.1}C_{3.2}$ represents a new type of structure of rare-earth boron carbides. The trigonal crystal structure [$a=b=23.710(9)A$, $c=6.703(2)A$, $P3m1$] is composed of alternate $[B_{1/3}C_{2/3}]$-Sc-C-Sc-$[B_{1/3}C_{2/3}]$ layers, with the boron and carbon mixed layer $[B_{1/3}C_{2/3}]$ forming a very rare graphitelike structure. Interesting characteristics of this compound were made clear.

The scandium-carbon-scandium layers could be removed from the graphitelike layers with the application of oxydic agents. This behavior is reminiscent of intercalants in GIC's. Furthermore, some physical properties investigated in this paper, namely, the anisotropic behavior of resistivity, the quadratic temperature dependence of the in-plane resistivity, and paramagnetic orbital susceptibility, are similar to that observed for GIC's. We conclude that this compound can be considered to be a new type of graphite intercalationlike compound. Up to now, hundreds of GIC's with conventional carbon graphite layers have been researched over the years, however, this is the first comprehensive report of a compound with a boron/carbon mixed layer exhibiting GIC-like properties.

The following features of this compound are of particular interest and promise exciting future developments.

First of all, the method of synthesizing the compound, a two-step sintering process, i.e., solid-state reaction, is largely different from typical GIC synthesis. Further study on the dynamics of the formation of the graphitelike structure of this compound may lead to the realization of a new family of graphite intercalationlike compounds.

Second, the graphitelike layer is composed of mixed boron and carbon atoms. Only three compounds have previously been reported to contain a [BC] graphitelike structure. Boron and carbon mixed graphitelike layers are very interesting in themselves for the following possible applications; as possible base materials for new fullerenes and possible high-spin molecular magnets, leading to applications as magnetic components. As we have noted above, the Sc-C-Sc layers could be removed from the compound yielding a graphitelike [BC] residue. This [BC] residue itself will be the object of further study.

Third, the intercalant layer of our compound is composed of a denser concentration of atoms than many other GIC's. The composition can be written as $2Sc_2C$-$(B_2C_4)_{1.1}$ (the fractional numbers are used for simplicity as the unit cell and the number of atoms inside it are very large). The C to guest atom ratio, or rather in this case, the graphitic atom to guest atom ratio, is roughly 1, which is quite small. Despite this, the compound has properties similar to GIC's and the guest layers can be removed from the graphitic layers. As noted above, further study on the dynamics of the formation of this structure may yield valuable information on high-density intercalation in GIC type compounds.

A further interesting characteristic was that a $\log T$ increase in resistivity and negative magnetoresistance was observed at low temperatures, indicative of 2D Anderson localization. We take the origin to be disorder in the boron and carbon graphitelike layer, possibly due to the singular composition of the $[B_{1/3}C_{2/3}]$ layer.

ACKNOWLEDGMENTS

The authors are grateful to Dr. E. Takayama-Muromachi for helping us with all the transport measurements. This work was partially supported by a Science and Technology Agency (STA) fund project.

*Email: moritk@nirim.go.jp

[1] M. S. Dresselhaus and G. Dresselhaus, Adv. Phys. **30**, 139 (1981).
[2] Y. Shi, A. Leithe-Jasper, L. Bourgeois, Y. Bando, and T. Tanaka, J. Solid State Chem. **148**, 442 (1999).
[3] M. Worle, R. Nesper, G. Mair, M. Schwarz, and H. G. V. Schnering, Z. Anorg. Allg. Chem. **621**, 1153 (1995).
[4] M. Worle and R. Nesper, J. Alloys Compd. **216**, 75 (1994).
[5] J. Kouvetakis, R. B. Kaner, M. L. Sattler, and N. Bartlett, J. Chem. Soc. Chem. Commun. **1986**, 1758.
[6] H. Kamimura, K. Nakao, T. Ohno, and T. Inoshita, Physica B & C **99**, 401 (1980).
[7] J. Kondo, Prog. Theor. Phys. **32**, 37 (1964).
[8] E. Abrahams, P. W. Anderson, D. C. Licciardello, and T. V. Ramakrishnan, Phys. Rev. Lett. **42**, 673 (1979).
[9] P. W. Anderson, E. Abrahams, and T. V. Ramakrishnan, Phys. Rev. Lett. **43**, 718 (1979).
[10] See, for example, C. Kittel, Quantum Theory of Solids (Wiley, New York, 1987); J. R. Schrieffer, J. Appl. Phys. **38**, 1143 (1967).
[11] M. Suzuki, C. Lee, I. S. Suzuki, K. Matsubara, and K. Sugihara, Phys. Rev. B **54**, 17 128 (1996).
[12] M. Suzuki, I. S. Suzuki, C. Lee, R. Niver, K. Matsubara, and K. Sugihara, J. Phys.: Condens. Matter **9**, 10 399 (1997).
[13] L. Piraux, V. Bayot, X. Gonze, J. P. Michenaud, and J. P. Issi, Phys. Rev. B **36**, 9045 (1987).
[14] L. Piraux, K. Amine, V. Bayot, J. P. Issi, A. Tressaud, and H. Fujimoto: Solid State Commun. **82**, 371 (1992).
[15] L. Piraux, V. Bayot, J. P. Issi, M. S. Dresselhaus, M. Endo, and T. Nakajima, Phys. Rev. B **41**, 4961 (1990); L. Piraux, V. Bayot, J. P. Issi, M. S. Dresselhaus, M. Endo, and T. Nakajima, *ibid.* **45**, 14 315 (1992).
[16] V. A. Kulbachinskii, S. G. Ionov, V. V. Avdeev, N. B. Brandt, S. A. Lapin, A. G. Mandrea, I. V. Kuzmin, and A. De Visser, J. Phys. Chem. Solids **57**, 893 (1996).
[17] L. Piraux, J. Mater. Res. **5**, 1285 (1990).
[18] S. Hikami, A. I. Larkin, and Y. Nagaoka, Prog. Theor. Phys. **63**, 707 (1980).
[19] S. A. Safran and F. J. DiSalvo, Phys. Rev. B **20**, 4889 (1979).
[20] J. Blinowski and C. Rigaux, Synth. Met. **8**, 241 (1983).